

Apatitic Deposition in Osteoblasts Cultured on Micropatterned Silicon

Kathryn Dorst¹, Michael Hadjiargyrou², and Yizhi Meng^{1*}

¹Department of Materials Science and Engineering, Stony Brook University, Stony Brook, NY, 11794-2275, USA

²Department of Life Sciences, New York Institute of Technology, Old Westbury, NY, 11568-8000, USA

*Corresponding author: Yizhi Meng, Department of Materials Science and Engineering, Stony Brook University, Stony Brook, NY, 11794-2275, USA, Tel: 1-631-632-8552; Fax: 1-631-632-8052; E-mail: Yizhi.Meng@StonyBrook.edu

Received date: 16 January 2014; Accepted date: 4 June 2014; Published date: 13 June 2014

Copyright: © 2014 Kathryn Dorst et al. This is an open-access article distributed under the terms of the Creative Commons Attribution License, which permits unrestricted use, distribution, and reproduction in any medium, provided the original author and source are credited.

Abstract

In this study, the osteogenic differentiation of murine pre-osteoblasts cultured on patterned silicon was investigated. Specifically, micropatterns were fabricated in <100> orientation silicon wafers to create linear gratings with a width of either 2 μm (2 μm depth, 10 μm pitch) or 20 μm (2 μm depth, 30 μm pitch). Two subclones (4, 24) of the MC3T3-E1 osteoblast-like cell line were seeded on the micropatterns and cultured in osteogenic induction medium for 28 days. Cells cultured on planar silicon served as the controls. Apatite formation was examined using synchrotron X-ray diffraction. Deposition of [002] and [211]/[112] apatite-like material was clearly observed in subclone 4 (strongly mineralizing) osteoblasts cultured on both micro patterns.

Keywords: Osteoblast; Micropatterns; Apatite; XRD

Introduction

The development of successful bone implants rests on a full understanding of cell-adhesion mechanisms under physiologically relevant conditions. This bottom-up approach focuses on the ability of material properties to guide the initial adsorption of extracellular matrix (ECM) proteins and, subsequently, cell proliferation, migration, differentiation and tissue morphogenesis [1]. The complex, intercalated pathways that are involved are still not completely understood, however the ECM is now recognized as a critical component in guiding complex cell-cell interactions in addition to being a structural scaffold [2].

In the last decade, synthetic implant technologies have been greatly improved by advancements in the field of bioMEMS (bio-microelectromechanical systems). First developed for computer microprocessors, MEMS have contributed to the progress of fundamental biological research as well as the development of medical devices [3,4]. Micropatterning techniques can greatly enhance the biocompatibility of synthetic biomimetic scaffolds and stimulate cell attachment and growth. Cells can be cultured either on the original micropatterns fabricated using standard photolithography followed by a dry etching process, or on elastomeric materials containing the inverse of the micro patterns transferred via soft lithography. These topographical features mimic those that would be present on the ECM and represent surface dimensions relevant to cell behavior in vivo. Several instances have shown that patterned ridges and grooves can promote cell adherence in fibroblasts and skeletal stem cells [5-13].

Micropatterned surfaces (ridges/grooves, dots) can also promote the adherence of osteoblasts and periodontal cells [6,7,9,12-16], however the extent of biomineral formation in these cell culture models has not been examined extensively. To the best of our knowledge, previous studies of osteoblast development on biomimetic substrates have been limited to the use of hydroxyapatite (HA)-containing bioactive ceramic coatings [17,18]. Because

microtopography can induce contact guidance [19], which is one of the critical steps in determining cytoskeletal development and gene/protein expression, we were motivated to investigate whether the manipulation of surface dimension alone is able to promote osteoblast differentiation without an a priori coating of bioceramic material. Increased understanding in the mineralization capacity of osteoblasts in response to external physical cues would help to devise strategies to increase the longevity of orthopaedic implant materials and improve tissue integration, while at the same time minimizing scar tissue formation and implant rejection [20].

Materials and Methods

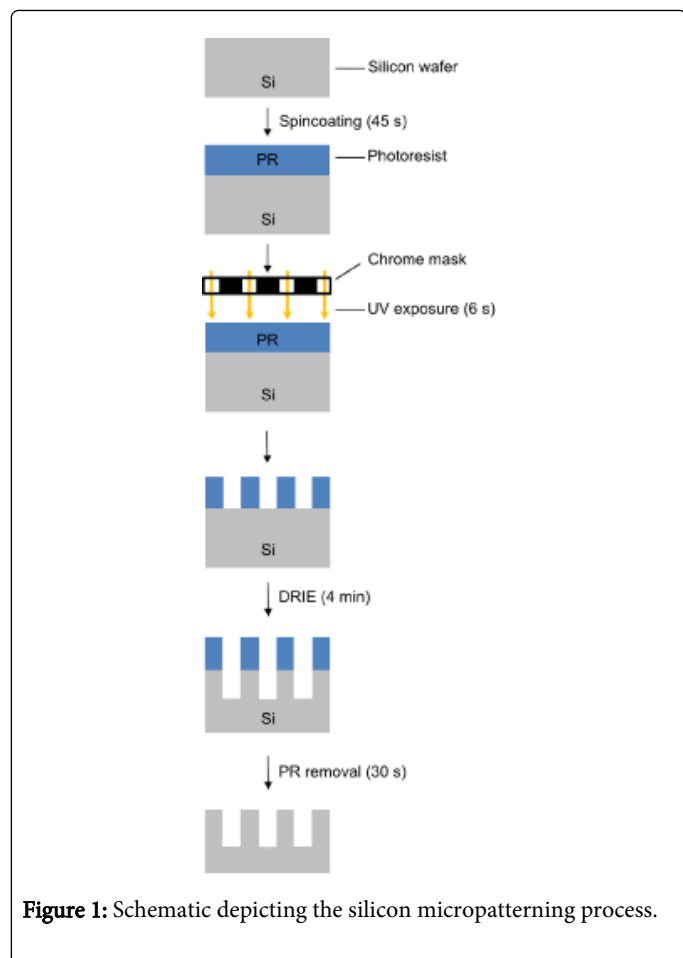
Substrate preparation

To pattern the silicon substrates, a positive photo resist, S1811 (Rohm and Haas), was first spin coated at 4000 RPM for 45 seconds onto a clean silicon wafer (<100> orientation, Silicon Quest International Inc., Santa Clara, CA). After prebaking at 110°C for 2 minutes, micro patterns were transferred onto the substrate using a chrome photo mask and a UV mask aligner (Figure 1). The exposed photo resist was developed using a 1:1 mixture of DI water: MF 312 developer (Rohm and Haas) for 30 seconds. Development was stopped by rinsing with DI water and drying with a gentle stream of nitrogen gas. A deep reactive ion etch (DRIE) was performed at 25°C for 4 minutes on an Oxford Instruments Plasma lab 100 (Oxfords hire, UK) until a depth of 2 μm was achieved. The remaining unexposed resist was removed with acetone, followed by DI water rinse and drying with nitrogen (Figure 1).

Cell culture and development

Strongly mineralizing (sub clone 4) and weakly mineralizing (sub clone 24) MC3T3-E1 osteoblast-like cells were maintained in MEM-α supplemented with 10% fetal bovine serum (FBS) and 1% penicillin-streptomycin. Cells were kept in an incubator at 37°C with 5% CO₂, 95% relative humidity. The silicon samples were first sterilized by autoclaving and cooled to room temperature before being transferred

aseptically to a sterile 24-well tissue culture plate. The substrate was then either directly exposed to cell culture medium or functionalized with a sterile 10 µg/mL solution of fibronectin for 30 minutes at room temperature, followed by rinsing with phosphate-buffered saline (PBS) and blocking with a solution of bovine serum albumin. Cells were then seeded at 50,000 cells/cm² and incubated for 24 hours at 37°C (5% CO₂, humidified) to attach completely and to reach confluency. To induce differentiation, medium was supplemented with 4 mM glycerol 2-phosphate and 50 µg/mL sodium L-ascorbate. Fresh induction medium was given every 2-3 days.



Scanning electron microscopy (SEM)

After 28 days of incubation, cellularized wafer samples were rinsed twice with phosphate-buffered saline (PBS) and DI water, fixed with 70% ethanol and air dried. Images were collected using a JEOL 7600 analytical SEM (15keV accelerating voltage) at the Center for Functional Nanomaterials, Brookhaven National Laboratory.

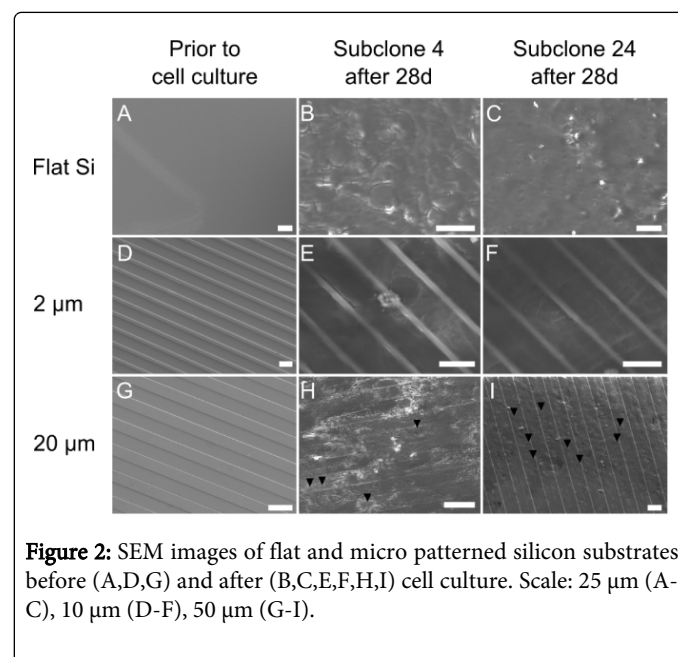
Synchrotron X-Ray diffraction (XRD)

Samples after 28 days of cell culture were fixed as described above for SEM. Synchrotron grazing incidence X-ray diffraction (GIXD) experiments were conducted at beam line X6B at the National Synchrotron Light Source (Brookhaven National Laboratory, Upton, NY) using focused X-ray beam at 0.65255Å wavelength (spot size: 0.25 mm high, 0.4 mm wide). Samples were mounted in air 150 mm from the detector screen. Grazing incidence diffraction patterns with

incident angle 0-2° were recorded using an X-ray CCD detector and calibrated using a standard Al₂O₃ powder plate. Two-dimensional false color images were collected from a CCD camera and converted to intensity profiles using the Data squeeze software. The volume-weighted size of [002] crystallites was measured using the Scherrer equation [21].

Results and Discussion

SEM images of both mineralizing (subclone 4) and non-mineralizing (subclone 24) MC3T3-E1 cells showed very dense cultures after 28 days of exposure to induction medium (Figure 2). The cells appeared more rounded than expected, particularly on the flat substrates (Figure 2B and 2C). This could be because only a mild fixative, ethanol, was used to avoid artifacts in the XRD data. On the 2 µm micropatterned Si, the osteoblasts appeared to have a larger spreading area, with numerous filopodia extending from many of the cells (Figures 2E and 2F). Clusters of biomineral were also observed in the subclone 4, but not subclone 24, cells, similar to previous reports [21]. On the 20 µm micropatterned Si, more cells were observed to be firmly attached on the ridges than in the valleys (arrowheads in Figures 2H and 2I).



Synchrotron XRD data showed that there was a very noticeable presence of both [002] and [211]/ [112] apatite peaks in the strongly mineralizing subclone 4 cultures on either the narrow (2 µm) or wide (20 µm) silicon micropatterns (Figure 3). For the weakly mineralizing subclone 24 cells, there was a complete absence of the [002] peak and a small [211]/[112] composite peak (Figure 3). These data differ from our previous results, which showed that subclone 24 cells failed to produce any mineral on planar silicon [21]. Because the substrates in the previous study were not functionalized with a fibronectin (Fn) pre-coating, we also investigated the role of Fn treatment in the current study. Our results showed that mineralizing subclone 4 cells cultured on planar silicon that is only functionalized with fibronectin produced no discernible XRD peaks associated with apatite deposition (Figure 3). Similarly, planar silicon that is not functionalized with Fn also did not induce mineralization in these cells after 28 days and produced a

nearly identical XRD spectrum (Figure 3). This can most probably be attributed to the fact that the cell culture medium contains ample amount of Fn that eventually adsorbs onto the silicon during the course of the experiment. Computed areas under the peaks confirmed that there was no apatite deposition in subclone 4 cells on flat silicon or in subclone 24 cells on the wide (20 μm) micropatterns. A very low amount of [211]/[112] HA was seen in the subclone 24 cells cultured on the narrow (2 μm) micropatterns. In contrast, subclone 4 cells deposited remarkably much more apatite on both micropatterns (Figure 4). Crystallite size calculated from the full-width-half-maximum of the [002] peak in the XRD spectra of subclone 4 cells was found to be 6.0 nm for apatite deposited on the wide (20 μm) micropatterns and 4.3 nm for apatite deposited on the narrow (2 μm) micropatterns.

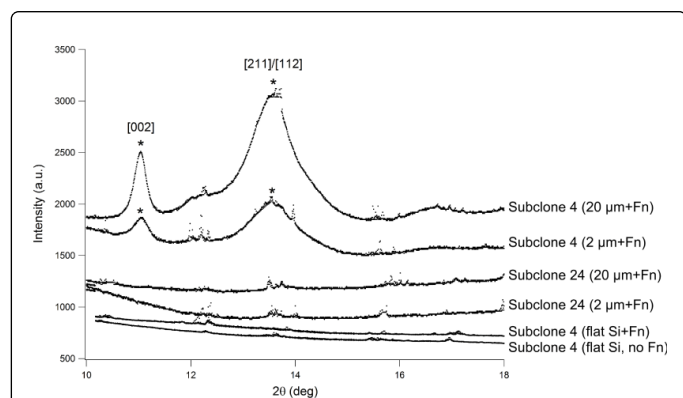


Figure 3: Synchrotron X-ray diffraction data for MC3T3-E1 subclone 4 and 24 osteoblasts cultured on narrow (2 μm width, 10 μm pitch, 2 μm depth) and wide (20 μm width, 30 μm pitch, 2 μm depth) micro patterned silicon, as well as planar silicon. Grazing incidence x-ray scattering was done using a $\lambda=0.65255 \text{ \AA}$ and beam energy of 19 keV.

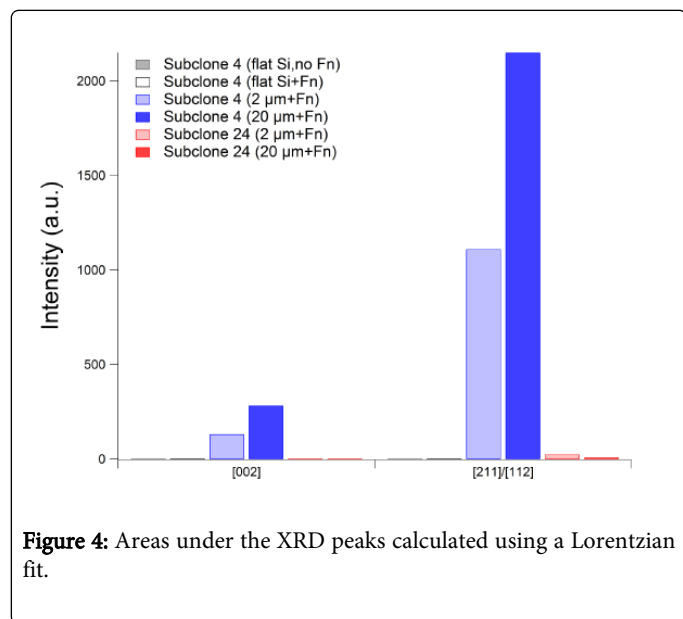


Figure 4: Areas under the XRD peaks calculated using a Lorentzian fit.

These results suggest that micro topography can indeed enhance the osteogenic differentiation of murine osteoblasts without an a priori

coating of bioceramic material. In the case of silicon, osteoblast mineralization does not appear to be modulated by the addition of a functionalized Fn coating. This may be partly due to the hydrophilic nature of native silicon oxide, and as such, the outcomes may be different if silicon is first treated with a hydrophobic polymer thin film such as sulfonated polystyrene, which has previously been shown to stimulate fibrillogenesis of ECM proteins [21]. Fibronectin supports cell adhesion and spreading, and affects the integration of tissue with orthopedic implants [22]. The early-stage protein-material interactions depend on the exposure of cell adhesive domains related to cell differentiation and greatly influence osteoblast mineralization [23-26]. For example, osteoblasts cultured on Fn physisorbed onto -NH₂ functionalized surfaces show favorable differentiation and mineralization [23-25], whereas on -COOH functionalized surfaces Fn inhibits differentiation and mineralization in osteoblasts [23,27,28]. Therefore, the (un) folding of Fn is extremely sensitive to minute changes in surface chemistry [29-31] and its self-association can be significantly perturbed by changes in wettability. An interesting question is whether or not surface microtopography and hydrophobic modification of the substrate surface have any additive effect on osteoblast differentiation, for which further research is needed to evaluate. Moreover, the inability of subclone 24 cells to mineralize may not only be dependent on disruptions in mechano transduction-associated pathways. To the best of our knowledge, this is the first observation of apatitic production in an osteoblast cell culture on micro patterned silicon using synchrotron XRD.

Conclusions

This study demonstrated the effect of micro patterning alone on apatite formation in an osteoblast cell culture. Our results show that deposition of an apatite-like material was possible without seeding the cells onto an a priori bioceramic layer. By varying the surface dimension of the silicon patterns, the osteogenic capacity of MC3T3-E1 murine osteoblasts was altered. This suggests that physical modulation of materials may be optimized to enhance the integration of bone tissue to silicon-based orthopaedic implants.

Acknowledgements

The authors are grateful to Dr. Aaron Stein for his help in the nanopatterning facility and to Dr. Elaine Dimasi for her assistance at beam line X6B. Research was carried out in part at the Center for Functional Nanomaterials and the National Synchrotron Light Source, Brookhaven National Laboratory, which is supported by the U.S. Department of Energy, Office of Basic Energy Sciences, under Contract No. DE-AC02-98CH10886.

References

1. Bruinink A, Bitar M, Pleskova M, Wick P, Krug HF, et al. (2014) Addition of nanoscaled bioinspired surface features: A revolution for bone-related implants and scaffolds. *Journal of Biomedical Materials Research Part A* 102: 275-294.
2. Daley WP, Peters SB, Larsen M (2008) Extracellular matrix dynamics in development and regenerative medicine. *J Cell Sci* 121: 255-264.
3. Bustillo JM, Howe RT, Muller RS (1998) Surface micromachining for micro electro mechanical systems. *Proceedings of the IEEE* 86: 1552-1574.
4. Fu G, Soboyejo WO (2009) Cell/surface interactions of human osteosarcoma (HOS) cells and micro-patterned poly dimethylsiloxane (PDMS) surfaces. *Materials Science and Engineering: C* 29: 2011-2018.

5. Chen CS, Mrksich M, Huang S, Whitesides GM, Ingber DE (1997) Geometric control of cell life and death. *Science* 276: 1425-1428.
6. Lee SW, Kim SY, Lee MH, Lee KW, Leesungbok R, et al. (2009) Influence of etched microgrooves of uniform dimension on in vitro responses of human gingival fibroblasts. *Clin Oral Implants Res* 20: 458-466.
7. Lee SW, Kim SY, Rhyu IC, Chung WY, Leesungbok R, et al. (2009) Influence of microgroove dimension on cell behavior of human gingival fibroblasts cultured on titanium substrata. *Clin Oral Implants Res* 20: 56-66.
8. Maeda YT, Inose J, Matsuo MY, Iwaya S, Sano M (2008) Ordered patterns of cell shape and orientational correlation during spontaneous cell migration. *PLoS One* 3: e3734.
9. Martinez E, Engel E, Lopez-Iglesias C, Mills CA, Planell JA, et al. (2008) Focused ion beam/scanning electron microscopy characterization of cell behavior on polymer micro-/nanopatterned substrates: a study of cell-substrate interactions. *Micron* 39: 111-116.
10. Miller C, Shanks H, Witt A, Rutkowski G, Mallapragada S (2001) Oriented Schwann cell growth on micropatterned biodegradable polymer substrates. *Biomaterials* 22: 1263-1269.
11. Pesen D, Haviland DB (2009) Modulation of cell adhesion complexes by surface protein patterns. *ACS Appl Mater Interfaces* 1: 543-548.
12. Sjöström T, Dalby MJ, Hart A, Tare R, Oreffo RO, et al. (2009) Fabrication of pillar-like titania nanostructures on titanium and their interactions with human skeletal stem cells. *Acta Biomater* 5: 1433-1441.
13. Su WT, Yang JY, Lin CD, Chu IM (2004) Control Cell Behavior on Physical Topographical Surface. *Japanese Journal of Applied Physics* 43: 3806-3809.
14. Lim JY, Dreiss AD, Zhou Z, Hansen JC, Siedlecki CA, et al. (2007) The regulation of integrin-mediated osteoblast focal adhesion and focal adhesion kinase expression by nanoscale topography. *Biomaterials* 28: 1787-1797.
15. Mussig E, Schulz S, Spatz JP, Ziegler N, Tomakidi P, et al. (2010) Soft micropillar interfaces of distinct biomechanics govern behaviour of periodontal cells. *Eur J Cell Biol* 89: 315-325.
16. Kim EJ, Boehm CA, Mata A, Fleischman AJ, Muschler GF, et al. (2010) Post microtextures accelerate cell proliferation and osteogenesis. *Acta Biomater* 6: 160-169.
17. Aniket, Young A, Marriott I, El-Ghannam A (2012) Promotion of pro-osteogenic responses by a bioactive ceramic coating. *J Biomed Mater Res A* 100: 3314-3325.
18. Rodríguez-Valencia C, Lopez-Alvarez M, Cochon-Cores B, Pereiro I, Serra J, et al. (2013) Novel selenium-doped hydroxyapatite coatings for biomedical applications. *J Biomed Mater Res A* 101 :853-861.
19. Dorst K, Rammelkamp D, Hadjiargyrou M, Gersappe D, et al. (2013) The effect of exogenous zinc concentration on the responsiveness of MC3T3-E1 pre-osteoblasts to surface microtopography: Part I (migration). *Materials* 6: 5517-5532.
20. Soboyejo WO, Nemetski B, Allameh S, Marcantonio N, Mercer C, et al. (2002) Interactions between MC3T3-E1 cells and textured Ti6Al4V surfaces. *J Biomed Mater Res* 62: 56-72.
21. Meng Y, Qin YX, DiMasi E, Ba X, Rafailovich M, et al. (2009) Biomimetic mineralization of a self-assembled extracellular matrix for bone tissue engineering. *Tissue Eng Part A* 15: 355-366.
22. Kilpadi KL, Chang PL, Bellis SL (2001) Hydroxylapatite binds more serum proteins, purified integrins, and osteoblast precursor cells than titanium or steel. *J Biomed Mater Res* 57: 258-267.
23. Keselowsky BG, Collard DM, Garcia AJ (2004) Surface chemistry modulates focal adhesion composition and signaling through changes in integrin binding. *Biomaterials* 25: 5947-5954.
24. Keselowsky B, Collard D, Garcia A (2005) Integrin binding specificity regulates biomaterial surface chemistry effects on cell differentiation. *Proceedings of the National Academy of Sciences of the United States of America* 102: 5953-5957.
25. Liu L, Chen S, Giachelli CM, Ratner BD, Jiang S (2005) Controlling osteopontin orientation on surfaces to modulate endothelial cell adhesion. *J Biomed Mater Res A* 74: 23-31.
26. Tidwell CD, Ertel SI, Ratner BD, Tarasevich BJ, Atre S, et al. (1997) Endothelial cell growth and protein adsorption on terminally functionalized, self-assembled monolayers of alkanethiolates on gold. *Langmuir* 13 :3404-3413.
27. Lan MA, Gersbach CA, Michael KE, Keselowsky BG, Garcia AJ (2005) Myoblast proliferation and differentiation on fibronectin-coated self assembled monolayers presenting different surface chemistries. *Biomaterials* 26: 4523-4531.
28. Lestelius M, Liedberg B, Tengvall P (1997) In vitro plasma protein adsorption on omega-functionalized alkanethiolate self-assembled monolayers. *Langmuir* 13: 5900-5908.
29. Baujard-Lamotte L, Noinville S, Goubard F, Marque P, Pauthe E (2008) Kinetics of conformational changes of fibronectin adsorbed onto model surfaces. *Colloids Surf B Biointerfaces* 63: 129-137.
30. Bergkvist M, Carlsson J, Oscarsson S (2003) Surface-dependent conformations of human plasma fibronectin adsorbed to silica, mica, and hydrophobic surfaces, studied with use of Atomic Force Microscopy. *J Biomed Mater Res A* 64: 349-356.
31. Gugutkov D, Altankov G, Rodríguez Hernández JC, MonleónPradas M, Salmerón Sánchez M (2010) Fibronectin activity on substrates with controlled --OH density. *J Biomed Mater Res A* 92: 322-331.